PHYSICAL REVIEW A **84**, 021807(R) (2011)

# Stationary nonlinear Airy beams

A. Lotti,[1,3] D. Faccio,[1,2,*] A. Couairon,[3] D. G. Papazoglou,[4,5] P. Panagiotopoulos,[4] D. Abdollahpour,[4,6] and S. Tzortzakis[4]

[1]*Dipartimento di Fisica e Matematica, Università del'Insubria, Via Valleggio 11, I-22100 Como, Italy*

[2]*School of Engineering and Physical Sciences, SUPA, Heriot-Watt University, Edinburgh EH14 4AS, United Kingdom*

[3]*Centre de Physique Théorique, CNRS, École Polytechnique, F-91128 Palaiseau, France*

[4]*Institute of Electronic Structure and Laser (IESL), Foundation for Research and Technology, Hellas (FORTH), P.O. Box 1527, GR-71110 Heraklion, Greece*

[5]*Materials Science and Technology Department, University of Crete, GR-71003 Heraklion, Greece*

[6]*Physics Department, University of Crete, GR-71003 Heraklion, Greece*

(Received 7 March 2011; published 22 August 2011)

We demonstrate the existence of an additional class of stationary accelerating Airy wave forms that exist in the presence of third-order (Kerr) nonlinearity and nonlinear losses. Numerical simulations and experiments, in agreement with the analytical model, highlight how these stationary solutions sustain the nonlinear evolution of Airy beams. The generic nature of the Airy solution allows extension of these results to other settings, and a variety of applications are suggested.

DOI: 10.1103/PhysRevA.84.021807 PACS number(s): 42.25.−p, 03.50.−z, 42.65.Jx

*Introduction.* Airy beams are a well-known family of stationary freely accelerating wave forms. Originally proposed in the context of quantum mechanics as a nonspreading solution to the Schrödinger equation for free particles [1], they were later proposed as optical wave packets with finite energy content [2,3]. The finite-energy Airy beam is characterized by a main intensity lobe that decays exponentially to zero on one side and decays with damped oscillations on the other. The interest for these beams lies in the fact that, if they have a sufficiently wide apodization, the main intensity lobe propagates free of diffraction while bending in the direction transverse to propagation or accelerating along the propagation direction if the temporal profile of the pulse is Airy shaped [4]. The ballisticlike properties of the Airy beam [5] lend it to particular applications such as optically mediated particle clearing [6] or generation of curved plasma filaments [7]. Recently a demonstration of light bullets using Airy cube wave packets (Airy in space and time) has also been reported [8]. Alongside the linear properties of Airy beams, nonlinear propagation of high-intensity Airy beams has also attracted attention [9,10]. It has been noted that upon increasing the Airy peak intensity the beam may either break up and emit a series of tangential emissions [11] or exhibit shrinking and modification of the Airy profile even below the critical threshold power for self-focusing [12,13]. Notably, Giannini *et al.* first described temporal self-accelerating solitons in Kerr media [14].

In this Rapid Communication we demonstrate the existence of stationary Airy-like solutions in the presence of third-order Kerr nonlinearity of any sign (i.e., focusing or defocusing) and, most importantly, even in the presence of nonlinear losses (NLLs). We perform an analytical analysis that describes the shape and main features of one-dimensional nonlinear Airy wave packets, i.e., monochromatic beams that exhibit a curved trajectory. The Kerr nonlinearity is shown to lead to a compression of the Airy lobes (for a focusing nonlinearity) and nonlinear losses lead to an imbalance of the incoming energy flux toward the main lobe which in turn induces a reduction in the contrast of the Airy oscillations. This finding is then verified in numerical simulations and experiments that show the spontaneous emergence of the main features of stationary nonlinear Airy beams.

*Analytical description.* We consider the propagation of a monochromatic beam of frequency $\omega_0$ in one spatial dimension. The electric field $\mathcal{E}(x,z,t)$ is decomposed into carrier and envelope as $\mathcal{E}(x,z,t) = E(x,z)\exp(-i\omega t + ik_0 z)$, where $k_0 = \omega_0 n_0/c$ is the modulus of the wave vector at $\omega_0$ and $n_0 = n(\omega_0)$ is the value of the refractive index at $\omega_0$. In the presence of nonlinearity, such as the Kerr effect and multiphoton absorption, propagation may be described by the nonlinear Schrödinger equation for the complex envelope of the field:

$$\frac{\partial E}{\partial z} = \frac{i}{2k_0}\frac{\partial^2 E}{\partial x^2} + ik_0\frac{n_2}{n_0}|E|^2 E - \frac{\beta^{(K)}}{2}|E|^{2K-2}E, \quad (1)$$

where the nonlinear Kerr modification of the refractive index is $\delta n = n_2|E|^2$, while $K$ and $\beta^{(K)} \geqslant 0$ are the order and the coefficient of multiphoton absorption, respectively.

In the case of linear propagation, Eq. (1) admits the Airy beam solution $E = \mathrm{Ai}(y)\exp[i\phi_L(y,\zeta)]$, whose intensity profile is invariant in the uniformly accelerated reference system defined by the normalized coordinates $\zeta = z/k_0 w_0^2$, $y = x/w_0 - \zeta^2/4$, with $\phi_L(y,\zeta) \equiv y\zeta/2 + \zeta^3/24$ and $w_0$ a typical length scale so that the acceleration or curvature is given by $1/2k_0^2 w_0^3$. We are interested in finding *stationary* nonlinear solutions to Eq. (1), in the above sense (invariant in the accelerated reference system), with boundary conditions compatible with the shape and properties of Airy beams, whose asymptotic behavior as $y \to \pm\infty$ reads [15]

$$\mathrm{Ai}(y) \sim |y\pi^2|^{-1/4}\sin(|\rho| + \pi/4) \quad \text{for} \quad y \to -\infty, \quad (2)$$

$$\mathrm{Ai}(y) \sim \frac{(y\pi^2)^{-1/4}}{2}\exp(-|\rho|) \quad \text{for} \quad y \to +\infty, \quad (3)$$

where $\rho = (2/3)\mathrm{sgn}(y)|y|^{3/2}$. We therefore impose the constraints of a weakly localized tail toward $y \to -\infty$ and an exponentially decaying tail toward $y \to +\infty$. Solutions,

*d.faccio@hw.ac.uk

 

hereafter called nonlinear Airy beams (NABs) must also match Airy beams in the absence of nonlinearity. We thus rewrite Eq. (1) in normalized units in the accelerated reference frame $(\zeta, y)$ as

$$\frac{\partial E}{\partial \zeta} - \frac{1}{2}\zeta \frac{\partial E}{\partial y} = \frac{i}{2}\frac{\partial^2 E}{\partial y^2} + i\gamma |E|^2 E - \alpha |E|^{2K-2} E, \quad (4)$$

The nonlinear parameters read as $\gamma = k_0^2 n_2 w_0^2 / n_0$ and $\alpha = \beta^{(K)} k_0 w_0^2/2$.

In order to find the shape of NABs, we consider the complex envelope $E = A(y)\exp[i\phi(y,\zeta)]$ with a $\zeta$-invariant modulus, substitute into Eq. (4), separate real and imaginary parts, and require that the $\zeta$ dependence of the phase be the same as that of linear Airy beams $\phi(y,\zeta) = \phi_L(y,\zeta) + \psi(y)$. The modulus $A(y)$ and nonlinear phase $\psi(y)$ satisfy

$$A'' - yA - (\psi')^2 A + 2\gamma A^3 = 0, \quad (5)$$

$$\psi' A^2 = 2\alpha \int_y^{+\infty} A^{2K} dy \equiv N_y, \quad (6)$$

where primes stand for $d/dy$. The left-hand side of Eq. (6) represents the net power flux $N_y$ per unit propagation length through a $y$ boundary of a semi-infinite domain $[y, +\infty)$ in the coaccelerating reference frame. Equation (6) imposes the requirement that the flux compensates for the power $N_y$ lost by nonlinear absorption within this domain. In the linear case, i.e., with no NLLs ($\alpha = 0$), there is no net energy flux ($\psi' = 0$) and phase fronts exhibit the curvature of Airy beams [1]. Nonlinear losses, assumed to be finite [16], increase from $N_{+\infty} = 0$ at $y \to +\infty$ to $N_{-\infty} \equiv 2\alpha \int_{-\infty}^{+\infty} A^{2K} dy$ at $y \to -\infty$, thereby establishing an additional curvature of the phase front in the weakly decaying tail of the beam, since $\psi' \to N_{-\infty}/A^2$, whereas the exponentially decaying tail has the curvature of the Airy beam. By introducing the variable $B(\rho) = A(y)|\rho|^{1/6}$, Eqs. (6) and (5) can be combined into a Newton-like equation governing the tail amplitude in the limit $y, \rho \to \pm\infty$:

$$\frac{\partial^2 B}{\partial \rho^2} \mp B = \frac{N_{\pm\infty}^2}{B^3} \quad \text{for} \quad \rho \to \pm\infty. \quad (7)$$

Equation (7) admits solutions in the form $B \sim \exp(-\rho)$ and $B^2(\rho) \sim B_{-\infty}^2[1 + C\sin(2|\rho|)]$ as $\rho \to \pm\infty$. The latter exhibits oscillations of finite amplitude around the mean value $B_{-\infty}$ and contrast $C \equiv (1 - N_{-\infty}^2/B_{-\infty}^4)^{1/2}$, decreasing as the amount of total losses increases. In the absence of nonlinear absorption ($N_{-\infty} \to 0$), it reduces to the asymptotics of Eq. (2) with maximum contrast $C = 1$. The contrast vanishes for $B_{-\infty}^2 = N_{-\infty}$, showing that no solution exist above a certain threshold of total losses.

In analogy with the physics of nonlinear Bessel beams [17], NABs can be viewed as Airy beams reshaped by nonlinear absorption and the Kerr effect, the former being responsible for the power flux from the weakly decaying tail toward the intense lobes where nonlinear absorption occurs and the latter of a nonlinear phase shift [18]. This is expressed by considering the NAB as an unbalanced superposition of two stationary Hankel beams, each carrying energy in the direction of, or opposite to the main lobe:

$$A(y)e^{[i\psi(y)]} = \frac{1}{2}\sqrt{\frac{-y}{3}} \sum_{l=1}^{2} a_l e^{(-1)^l i\pi/6} H_{1/3}^{(l)}(|\rho|) \quad (8)$$

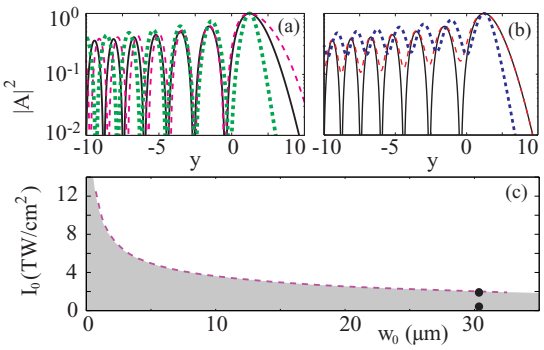


FIG. 1. (Color online) Nonlinear Airy wave forms for (a) a pure Kerr focusing (green dotted line) and defocusing (red dashed line) nonlinearity with no NLLs; (b) NLLs alone with $K = 5$ (red dashed line) and Kerr + NLLs (blue dotted line). (c) Domain of existence (shaded region) of the NAB solution in the case of water at $\lambda_0 = 800$ nm as a function of peak intensity and width of the linear solution. The circles indicate the peak intensities at which numerical simulations were performed (Fig. 2).

The power fluxes associated with each Hankel component exactly compensate for the balanced superposition with $a_1 = a_2 = 1$, which gives the stationary Airy beam with no net power flux. Unbalancing creates a net flux associated with a lowering of the contrast of the oscillating tail.

We numerically integrated Eqs. (6) and (5) from $+\infty$ to $-\infty$ starting from the linear asymptotic solution as a boundary condition in order to retrieve the intensity and phase profiles of the NAB. Figure 1(a) shows the normalized intensity profiles in the pure Kerr case, i.e., $\alpha = 0$, for focusing ($\gamma > 0$) and defocusing ($\gamma < 0$) Kerr nonlinearity, respectively. The width of the main lobe is narrower or wider depending on the sign of $\gamma$. Since the reference system in which we are considering the solutions is always referred to the linear case, the nonlinear solution preserves the same acceleration although the relation between the width of the main lobe and the peak acceleration no longer holds. In Fig. 1(b) for the $K = 5$ case and $\gamma = 0$ (red dashed line), we show the effect of multiphoton absorption and we observe a reduction of the contrast in the decaying oscillations, which asymptotically goes to $C$, and this reduction is greater when the total amount of energy lost in absorption (proportional to $N_{-\infty}$) is greater (data not shown). When we have both Kerr nonlinearity and multiphoton absorption, we observe features characteristic of both regimes (blue dotted line). As in the pure Kerr case, the acceleration of linear Airy beams is preserved. We performed a scan in the parameter space in order to derive the region of existence of these stationary solutions.

Figure 1(c) shows this domain in the $(I_0, w_0)$ coordinates for water at $\lambda_0 = 800$ nm (we considered $n_2 = 2.6 \times 10^{-16}$ cm$^2$/W, $n_0 = 1.3286$, $K = 5$, and $\beta^{(K)} = 8.3 \times 10^{-50}$ cm$^7$/W$^4$ [19]), where $I_0$ is the maximum intensity of the nonlinear profile and $w_0$ is the width of the corresponding linear solution, which represents the acceleration as $a(w_0) = 1/2k_0^2 w_0^3$.

*Nonlinear Airy beam evolution.* A relevant question is whether one is actually able to excite or experimentally observe stationary NABs. The ideal beams described above have infinite energy whereas experiments obviously resort

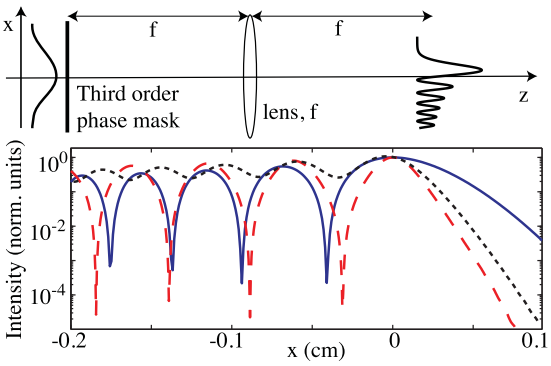


FIG. 2. (Color online) Numerical results: propagation in water with focal length $f = 20$ cm. Solid blue line, linear Airy profile; dashed red line, nonlinear Airy profile; black dotted line, nonlinear case with artificially increased NLLs. All profiles are shown in the focal plane of lens $f$ ($z = 20$ cm).

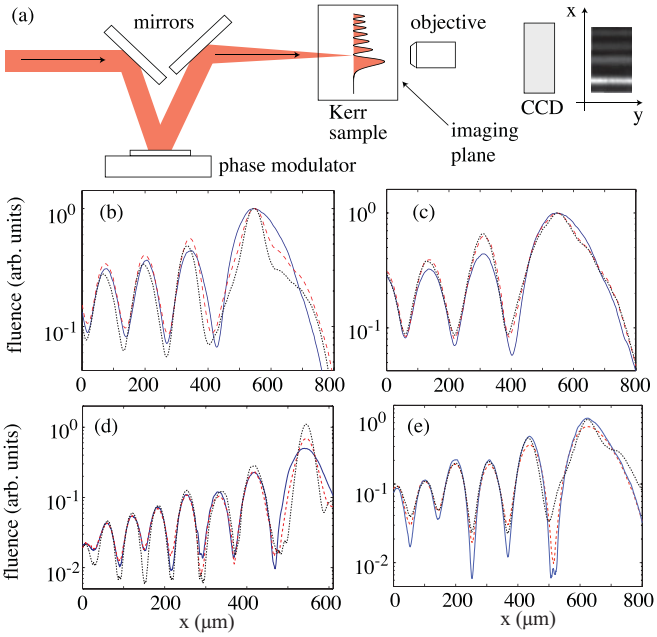


FIG. 3. (Color online) Experimental results: (a) Experimental layout. (b)–(e) Output Airy beam fluence profiles in logarithmic scale.(b) Water at three input energies 25 nJ (solid line), 350 $\mu$J (dashed line), and 530 (dotted line) $\mu$J and for an input Airy pulse with a main lobe FWHM of 159 $\mu$m. (c) Water at same energies as in (b) and a main lobe FWHM of 182 $\mu$m. (d) PMMA at three input energies 25 nJ (solid line), 78 $\mu$J (dashed line), and 196 (dotted line) $\mu$J and for an input Airy main lobe FWHM of 78 $\mu$m. (e) PMMA at same energies as in (d) and a main lobe FWHM of 136 $\mu$m.

to finite-energy realizations that cannot guarantee perfect stationarity. However, as in the linear case in which finite-energy Airy beams still exhibit the main stationary features, e.g., subdiffractive propagation of the main intensity peak, over a limited distance [2], we may expect the nonlinear Airy beam to emerge during propagation in the nonlinear regime. The rationale behind this reasoning is also based on the observation that stationary wave forms have been shown to act as attractor states for the dynamical evolution of laser beams and pulses in the nonlinear regime, e.g., dynamically evolving $X$ waves during ultrashort laser pulse filamentation [20,21], nonlinear unbalanced Bessel beams during the evolution of high-intensity Bessel beams [17,22], and the spatial Townes profile during the self-focusing of intense Gaussian pulses [23].

We performed a series of numerical simulations, solving Eq. (1) for the same material parameters as in Fig. 1 with an input Airy beam defined as in the linear regime, for various increasing input intensities. The Airy beam was generated by applying a third-phase mask to a Gaussian beam (full width at half maximum of 0.5 mm) followed by a $2 - f$ linear propagation so as to obtain the Fourier transform in the focal plane of the lens (focal length $f = 20$ cm). This layout is shown at the top of Fig. 2. In Fig. 2 we show a line-out of the nonlinear profile (dashed red line) obtained by numerical simulations based on Eq. (1), at $z = 20$ cm from the last focusing lens for $I_0 = 2$ TW/cm$^2$. The linear Airy profile (solid blue line) is included for comparison. The contraction of the main lobe and the different periodicity of the side lobes is clearly evident, while the effect of NLLs (i.e., loss of contrast in the side-lobe oscillations) is not observed. We therefore performed an additional simulation (black dotted line) at the same peak intensity with an increased nonlinear absorption coefficient, $\beta^{(K)} = 8.3 \times 10^{-45}$ cm$^7$/W: the strong reduction in the contrast of the Airy beam oscillations is now clear, indicating the presence of an inward flux that is stabilizing the energy loss in the main lobe.

*Experiments.* We performed two series of experiments by launching one-dimensional Airy beams with increasing input energy into two different nonlinear media: (1) a 2-cm-thick cuvette filled with water and (2) a 2.5-cm-thick sample of the polymer polymethyl-methacrylate (PMMA). The experimental setup is shown in Fig. 3(a): a third -order spatial phase, together with a quadratic one corresponding to a cylindrical Fourier lens, is impressed onto a Gaussian-shaped beam delivered by an amplified Ti:sapphire laser with 35 fs pulse duration, using a spatial light modulator (Hamamatsu LCOS). The Airy-shaped beam then propagates through the nonlinear sample and the beam profile at the exit surface is imaged onto a CCD camera. Figure 3(b) shows the spatial fluence profiles (in logarithmic scale) for three different input energies 25 nJ (linear propagation), 350 $\mu$J, and 530 $\mu$J and for an input phase profile such that the linear Airy main lobe full width at half maximum (FWHM) is 159 $\mu$m. The main lobe undergoes an evident contraction that increases with increasing energy, in agreement with the prediction summarized in Fig. 1(a) for the Kerr-dominated NAB. We then repeated the measurements with an increased input phase such that the Airy main lobe has a FWHM of 182 $\mu$m. Figure 3(c) shows the results for the same energies as in Fig. 3(b). The reduced density of the Airy peaks and the correspondingly lower spatial intensity gradients imply that now both self-focusing effects and the energy flux within the beam are weaker. We may therefore expect the effects of NLLs to become more evident. Indeed, while Kerr self-focusing effects are nearly absent, the contrast in the secondary Airy lobes decreases in agreement with the expected behavior of the "unbalanced" Airy beam, as summarized in Fig. 1(b). These effects are even more pronounced in measurements performed in PMMA which is

expected to have higher NLLs due to the lower multiphoton absorption photon number, $K = 3$. As for the case of water, two different Airy widths were tested, 78 $\mu$m [Fig. 1(d)] and 159 $\mu$m [Fig. 1(e)], at three different energies 25 nJ, 78 $\mu$J, and 246 $\mu$J, with similar dynamics as in water and with the larger Airy peak leading to increased NLL effects. We observe an increase of minimum intensity values by nearly an order of magnitude with increasing input energy. Although we do not have the same resolution and dynamic range as in the numerics, the experiments clearly show the predicted trends for the stationary NAB.

*Conclusions.* In conclusion, we have demonstrated the existence of a freely accelerating solution in the nonlinear regime that remains stationary even in the presence of nonlinear losses. Clearly these results may be extended to the original quantum context in which Airy wave packets were proposed for the first time [1]. NABs could also find practical applications in a similar fashion to stationary Bessel beams where the beam stability above ablation intensities has led to technical improvements in micromachining optical materials [24] or soft tissue laser surgery by using them as razor blades with a well-defined curvature. Stationarity is also a critical issue in "analog Hawking" emission experiments [25]: the nonlinear Airy beam may be used to reach huge $\sim 10^{21}$ m/s$^2$ accelerations and thus investigate related photon emission mechanisms [26].

[1] M. V. Berry *et al.*, Am. J. Phys. **47**, 264 (1979).
[2] G. A. Siviloglou *et al.*, Phys. Rev. Lett. **99**, 213901 (2007).
[3] G. A. Siviloglou *et al.*, Opt. Lett. **32**, 979 (2007).
[4] A. Chong *et al.*, Nature Photon. **4**, 103 (2009).
[5] G. A. Siviloglou *et al.*, Opt. Lett. **33**, 207 (2008).
[6] J. Baumgartl *et al.*, Nature Photon. **2**, 675 (2008).
[7] P. Polynkin *et al.*, Science **324**, 229 (2009).
[8] D. Abdollahpour *et al.*, Phys. Rev. Lett. **105**, 253901 (2010).
[9] S. Jia *et al.*, Phys. Rev. Lett. **104**, 253904 (2010).
[10] I. Kaminer *et al.*, Phys. Rev. Lett. **106**, 213903 (2011).
[11] P. Polynkin *et al.*, Phys. Rev. Lett. **103**, 123902 (2009).
[12] R-P. Chen *et al.*, Phys. Rev. A **82**, 043832 (2010).
[13] J. Kasparian and J.-P. Wolf, J. Europ. Opt. Soc. Rap. Public. **4**, 09039 (2009).
[14] J. A. Giannini *et al.*, Phys. Lett. A **141**, 417 (1989).
[15] *Handbook of Mathematical Functions*, edited by M. Abramowitz and I. Stegun (Dover, New York, 1972).
[16] With Airy beams, NLLs are finite only for $K > 2$.
[17] M. A. Porras *et al.*, Phys. Rev. Lett. **93**, 153902 (2004).
[18] P. Polesana *et al.*, Phys. Rev. E **73**, 056612 (2006).
[19] A. Dubietis *et al.*, Appl. Phys. B **84**, 439 (2006).
[20] M. Kolesik *et al.*, Phys. Rev. Lett. **92**, 253901 (2004).
[21] D. Faccio *et al.*, Phys. Rev. Lett. **96**, 193901 (2006).
[22] P. Polesana *et al.*, Phys. Rev. Lett. **99**, 223902 (2007).
[23] K. D. Moll *et al.*, Phys. Rev. Lett. **90**, 203902 (2003).
[24] M. K. Bhuyan *et al.*, Appl. Phys. Lett. **97**, 081102 (2010).
[25] F. Belgiorno *et al.*, Phys. Rev. Lett. **105**, 203901 (2010).
[26] P. G. Thirolf *et al.*, Eur. Phys. J. D **55**, 379 (2009).